

Statics and Dynamics of Condensed DNA within Phages and Globules

Theo Odijk*

Theory of Complex Fluids

Faculty of Applied Sciences

Delft University of Technology

Delft, the Netherlands

Abstract

Several controversial issues concerning the packing of linear DNA in bacteriophages and globules are discussed. Exact relations for the osmotic pressure, capsid pressure and loading force are derived in terms of the hole size inside phages under the assumption that the DNA globule has a uniform density. A new electrostatic model is introduced for computing the osmotic pressure of rodlike polyelectrolytes at very high concentrations. At intermediate packing, a reptation model is considered for DNA diffusing within a toroidal globule. Under tight packing conditions, a model of Coulomb sliding friction is proposed. A general discussion is given of our current understanding of the statics and dynamics of confined DNA in the context of to the following experiments: characterization of the liquid crystalline phases, X-ray scattering by phages, osmotic stress measurements, cyclization within globules and single-molecule determination of the loading forces.

*E-mail: odijktcf@wanadoo.nl;

Address for correspondence:

T. Odijk, P.O. Box 11036, 2301 EA Leiden, the Netherlands

1. Introduction

The compaction of DNA in biological cells and viruses presents us with rather unconventional problems in the physics of soft matter. In the case of phages or viruses, the DNA may be so close-packed that the thermodynamics is no longer extensive because it is dominated by the energy arising from regions of tight bending (Odijk 1998). Thus we are dealing with a defect rather than a bulk system. Confronting the mathematical physics of the DNA configurations as such is a formidable undertaking. Still, the condensed DNA globule ought to have relatively minor fluctuations in the density (Ubbink & Odijk 1996) so that simplified analyses are possible.

A general maxim in theoretical biology is not to theorize before one has assimilated pertinent data and the same would seem to apply to the field of DNA compaction also. In setting up the computations outlined here, I have relied heavily on what we have learned from a number of recent experiments. The spoollike structure of DNA in T7 and T4 bacteriophages has been established in a quantitative fashion (Cerritelli et al 1997; Olson et al 2001). For the phi29 phage we now have a fairly good comprehension of the connector motor (Simpson et al 2000) and the typical forces involved in DNA packaging as a function of length reeled in (Smith et al 2001). Cyclization experiments (Jary & Sikorav 1999) of DNA in condensed globules allow us to estimate the local friction the DNA coil experiences in a congested environment.

Provisional theories for DNA compacted in phages were already proposed a couple of decades ago (Reimer & Bloomfield 1978; Gabashvili et al 1991; Gabashvili & Grosberg 1992). Nevertheless, the notion that the tight curvature of the DNA sheath surrounding a hole determines the interaxial spacing, was stressed only recently (Odijk 1998). Theoretical activity in this area is currently gaining momentum but will be discussed in the last section. The experimental literature on DNA packaging in phages and viruses is vast and complicated and, owing to space limitations, cannot be dealt with here (for recent reviews of the experimental situation, see Grimes et al (2002) and Jardine & Anderson (2003)). Here I wish to emphasize several theoretical issues that have not been focussed on before.

A continuum approximation of the curvature energy of DNA condensed within a capsid is derived in terms of the inhomogeneous DNA density in the limit of small fluctuations. A further useful approximation for close packed DNA is to let the density be constant.

It turns out that it is then possible to derive general nanothermodynamic relations for quantities like the osmotic pressure, force of insertion, etc. Owing to the very high degree of packing in phages, we are obliged to reinvestigate the classical cell model for rodlike polyelectrolytes. The interpretation of the cyclization experiments of linear globular DNA leads to the (surprising?) conclusion that simple reptation seems to be valid though I note that regions of tight curvature are often absent in globules. The friction of DNA in highly congested phages is discussed in terms of current thinking on sliding friction at nanoscales. In the last section, I confront these new computations as well as previous theoretical work with the experiments mentioned above.

2. Continuum approximations

The persistence length of DNA is generally of the order of magnitude of the typical size of bacteriophages. This makes the statistical treatment of DNA viewed as a confined wormlike chain with self-interaction very difficult. Fortunately, there is one limit where we can make considerable headway, viz. when the DNA is close-packed at moderate to high densities owing to bending stresses. Such a condensed state may exhibit so-called frustration because the packing - hexagonal for instance - cannot be perfect (Earnshaw & Harrison 1977; Pereira & Williams 2000), but this effect will be neglected here.

Let us then consider a configuration of a DNA molecule enclosed within a capsid of volume V_0 and defined by the radius vector $\vec{r}(s)$ as a function of the contour distance s from one end. The bending energy U_c in a Hookean approximation is written in terms of the local radius of curvature $R_c(s)$ of the DNA curve at s (Yamakawa 1971)

$$U_c = \frac{1}{2} P k_B T \int_0^L ds \frac{1}{R_c^2(s)} \quad (1)$$

Here, the bending force constant equals $P k_B T$ where P is the DNA persistence length, k_B is Boltzmann's constant and T is the temperature. We wish to introduce the normalized density of DNA segments at position \vec{r} expressed in terms of a delta function

$$\rho_c(\vec{r}) = \frac{N}{L} \int_0^L ds \delta(\vec{r} - \vec{r}(s)) \quad (2)$$

$$\int d\vec{r} \rho_c(\vec{r}) = N$$

The contour length L of the DNA consists of N "segments" of length A , the distance between elementary charges viewed along the DNA helical axis. We next insert the density into eq (1) and average over all configurations (denoted by $\langle \ \rangle$) which is possible because $\vec{r}(s)$ is a unique nonintersecting curve.

$$\begin{aligned} \langle U_c \rangle = U &= \frac{1}{2} P A k_B T \int d\vec{r} \left\langle \frac{\rho_c(\vec{r})}{R_c^2(\vec{r})} \right\rangle \\ &\simeq \frac{1}{2} P A k_B T \int d\vec{r} \frac{\rho(\vec{r})}{R^2(\vec{r})} \end{aligned} \quad (3)$$

We have also introduced a close-packing approximation $\langle \rho_c(\vec{r})/R_c^2(\vec{r}) \rangle \simeq \langle \rho_c \rangle \langle R_c^{-2} \rangle \equiv \rho(\vec{r}) R^{-2}(\vec{r})$ which is certainly accurate when the DNA undulations away from the average are small. I note that eq (3) pertains to both purely mechanical and statistical mechanical types of theories. Even in the former, we still need to average over all configurations, for the capsid has a complicated shape so there must be a host of DNA conformations of virtually identical energies. The bending energy given by eq (3) was used recently (Odijk and Slok 2003) to set up a simple density functional theory of packing and will be commented on below.

Next, we consider a more severe approximation by letting the density be constant. It is conveniently expressed in terms of the area S of the unit cell of the packaged DNA ($\rho_0 \equiv 1/SA$) which we often take to be hexagonal. The supposition of uniform density allows us to deduce expressions of some generality. The bending energy is rewritten as

$$U = \frac{P k_B T}{2S} \int_{V_i}^{V_0} d\vec{r} R^{-2}(\vec{r}) \quad (4)$$

where the infinitesimal volume $d\vec{r} \equiv S ds$. The volumes V_i and V_0 are the inner and outer volumes, respectively, enclosing the packed DNA (see fig 1). We assume there is only one hole though it is stressed that general shapes of the capsid and hole are allowed. Now it can be argued by scaling and other arguments (Odijk 1986; Selinger & Bruinsma 1991; Kamien et al 1992) that the twist and splay contributions to the free energy of a tightly packed liquid crystal are small compared with the bending energy. Thus we interpret R^{-2} as an energy density of pure bending which depends on the director $\vec{n}(\vec{r})$ but not on S , the size of the unit cell. Moreover, because there should be no hairpins at close packing, the DNA mesophase is splayless at constant density (de Gennes 1977).

There is also a free energy of the DNA interacting with itself. We omit minor curvature and surface contributions (Ubbink & Odijk 1995) and express this energy as an extensive form proportional to the contour length L

$$F_{int} = Lf(S) \quad (5)$$

This pertains to a hypothetically straightened DNA lattice. Accordingly, we now want to minimize the total free energy

$$F_{tot} = U + F_{int} \quad (6)$$

subject to a volume constraint

$$V_i = V_0 - LS \quad (7)$$

We minimize F_{tot} with respect to the director \vec{n} (implicit in R^{-2}) and to the cell size S , keeping the outer volume V_0 fixed but also the chemical potentials of the small ions of the buffer in the reservoir containing the phage.

$$\left. \frac{\delta F_{tot}}{\delta \vec{n}} \right|_{S, V_i(S)} = 0 \quad (8)$$

$$\left. \frac{\partial F_{tot}}{\partial S} \right|_{\vec{n}} = 0$$

These expressions yield

$$Lf'(S) - \frac{U}{S} + \frac{P}{2S} \int_{A_i} d\vec{r}_i R_m^{-2}(\vec{r}_i) \left| \frac{\partial \vec{l}(\vec{r}_i)}{\partial S} \right| = 0 \quad (9)$$

in terms of an optimized inverse square radius of curvature R_m^{-2} and an integral over the surface of the inner hole (see fig 2). A variation in S induces a change in the vector \vec{l} at point \vec{r}_i , pointing normal to the inner surface in the direction of the hole. The variation of the inner volume can be similarly written with the help of eq (7)

$$\frac{\partial V_i}{\partial S} = - \int_{A_i} d\vec{r}_i \left| \frac{\partial \vec{l}(\vec{r}_i)}{\partial S} \right| = -L \quad (10)$$

Hence, it is expedient to define a measure of the hole size given by

$$E_i^{-2} \equiv \frac{\int_{A_i} d\vec{r}_i R_m^{-2}(\vec{r}_i) \left| \frac{\partial \vec{l}(\vec{r}_i)}{\partial S} \right|}{\int_{A_i} d\vec{r}_i \left| \frac{\partial \vec{l}(\vec{r}_i)}{\partial S} \right|} \quad (11)$$

Noting that $-f'(S)$ is simply the osmotic pressure π_{os} , we finally attain the nanothermodynamic relation

$$\pi_{os} = -\frac{U}{SL} + \frac{Pk_B T}{2SE_i^2} \quad (12)$$

The usual thermodynamics does not hold: if the hole is small, we have $V_0 = \mathcal{O}(SL)$ and $U = \mathcal{O}(PV_0^{1/3}k_B T/S)$ and so the osmotic pressure is not a purely intensive quantity.

Next, the average pressure \mathcal{P} on the capsid wall exerted by the DNA is computed by considering a virtual change in V_0 . Concomitantly, the director configuration $\vec{n}(\vec{r})$, the inner volume $V_i(V_0, S)$ and cell size S also change in such a way that the free energy remains a minimum (eq 8) and the constraint (eq 7) is obeyed. The resulting analysis is similar to that given above, leading to

$$\mathcal{P} = -\frac{\partial F_{tot}}{\partial V_0} = -\frac{\partial U}{\partial V_0} \Big|_S = \frac{Pk_B T}{2SE_i^2} - \frac{Pk_B T}{2SE_0^2} = \frac{U}{SL} + \pi_{os} - \frac{Pk_B T}{2SE_0^2} \quad (13)$$

The typical size E_0 of the capsid is defined via its surface similarly to eq (11). I note that this pressure is not at all identical to the osmotic pressure as one might have naively surmised.

It is also interesting to study a quasistatic force \mathcal{F} (in the absence of dissipative losses; Kindt et al 2001) upon increasing the length of DNA in the capsid. We require local equilibrium (eqs (14)) as \vec{n} , S and $V_i(S, L)$ adjust to the changing degree of packing subject to eq (13). It is straightforward to show that the "pressure" \mathcal{F}/S of insertion is given by

$$\frac{|\mathcal{F}|}{S} = \frac{\partial F_{tot}}{S\partial L} = \frac{f}{S} + \pi_{os} + \frac{U}{SL} \quad (14)$$

Again, it would have been difficult to anticipate this expression. We have derived eqs (12-14) for a phage of general shape at the expense of introducing the capsid and hole sizes as unconventional averages.

3. Hexagonal DNA lattice at high concentrations

We have argued that we merely need the free energy per unit length $f(S)$ of a straightened DNA lattice in order to evaluate pertinent quantities of the DNA enclosed in a capsid. In this section we assume such a lattice is perfectly hexagonal without defects. Actually, the DNA chains also undulate about a reference configuration but this effect is temporarily disregarded. The lattice model for rodlike polyelectrolytes is, of course, well known (Oosawa 1971), but the usual cell model which disposes of the hexagonal symmetry, breaks down

at high degrees of packing when the polyion cylinders are close. A new approximation is introduced here, though some general features of the Donnan equilibrium need to be discussed first.

For now, the lattice is free from simple electrolyte and consists of parallel cylindrical polyions together with attendant counterions dissolved in the water in the intervening void. In some model or approximation one introduces, there is generally an interface or line of symmetry where the negative electrostatic potential is a maximum and is set equal to zero. The electric field vanishes so the osmotic pressure π_{os} and chemical potential of the ions μ_i reduce to (Israelachvili 1985)

$$\begin{aligned}\pi_{os} &= \bar{\rho}_i k_B T \\ \mu_i &= \mu_{ref} + k_B T \ln \bar{\rho}_i\end{aligned}\tag{15}$$

where $\bar{\rho}_i$ is the concentration of counterions at the interface. We restrict ourselves to monovalent ions bearing an elementary charge q which are ideal save for their Coulombic interaction mediated by a supposedly uniform permittivity ϵ .

Next, the lattice is brought into thermodynamic contact with a large reservoir containing monovalent salt of concentration c_s . The activity coefficients of the small ions are set equal to unity so the resulting Donnan equilibrium, due to the equality of the chemical potentials of the small ions in the respective phases, yields

$$\rho_-(\bar{\rho}_i + \rho_+) = c_s^2\tag{16}$$

The polyelectrolyte suspension contains positive and negative ions arising from the simple salt, whose densities must be set equal in view of electroneutrality ($\rho_+ = \rho_-$). Therefore, upon eliminating ρ_+ and ρ_- , the osmotic pressure is simply (Oosawa 1971)

$$\begin{aligned}\pi_{os} &= (\bar{\rho}_i + \rho_+ + \rho_- - 2c_s)k_B T \\ &= \bar{\rho}_i k_B T g(w) \\ g(y) &\equiv (1 + y^2)^{1/2} - y \\ w &\equiv 2c_s/\bar{\rho}_i\end{aligned}\tag{17}$$

In the so-called cell model (developed by Fuoss, Katchalsky, Oosawa and others, see Oosawa 1971), the counterion concentration $\bar{\rho}_i$ at the interface in the salt-free case is given by

$$\bar{\rho}_i \simeq \frac{A\rho_0}{2Q}\tag{18}$$

This is valid at low and intermediate concentrations. For DNA, we have a segment length $A = 0.17$ nm and the Bjerrum length $Q = q^2/\epsilon k_B T = 0.71$ nm at room temperature implying that a fraction of counterions appears to be associated with the DNA rods. This is often termed counterion condensation (Manning 1969).

We now address the Poisson-Boltzmann equation in the lattice at high concentrations (in the salt-free case). The ion distribution $\rho(\vec{r})$ is connected to the (negative) electric potential φ via a Boltzmann distribution

$$\rho_i = q\bar{\rho}_i \exp(-q\varphi/k_B T) \quad (19)$$

which is inserted in the Poisson equation

$$\Delta\varphi = -\frac{4\pi\rho_i}{\epsilon} \quad (20)$$

This procedure is not entirely rigorous although it is quite accurate for monovalent ions (the difficulty is that the two densities in eqs (19) and (20) are very similar though not identical; see Fixman 1979).

Let us consider the case when the surfaces of the polyion cylinders are separated by only a short distance h which is much smaller than the cylinder radius a (see fig 3). Hansen et al (2001) then still insist on using a cell model in which the effect of the rods surrounding a test rod is mimicked by a cylindrical boundary. This seems a rather severe approximation. An alternative is to view the hole enclosed within the triangle in fig 3 as a separate entity which is feasible provided the electrostatic screening is sufficiently high. Solving the Poisson-Boltzmann equation in this geometry is still difficult, so we replace the hole by three sections involving thin layers of electrolyte, and one effective hollow cylinder whose radius b is appropriately chosen. I consider the latter first. The boundary condition for the electric field at its surface is

$$\left. \frac{d\varphi}{dr} \right|_b = \frac{4\pi\sigma_q}{\epsilon} \quad (21)$$

with r the radial coordinate. The negative charge density $\sigma_q = -q\sigma$ with σ the number of charges per unit area to be chosen below. We have to solve eq (19) and (20) so it is convenient to introduce the dimensionless variables $\Psi \equiv q\varphi/k_B T$ and $\bar{r} \equiv r/\lambda$ where the screening length λ is analogous to the Debye length

$$\lambda^{-2} \equiv 4\pi Q\bar{\rho}_i \quad (22)$$

The counterion density $\bar{\rho}_i$ now pertains to the centreline of the cylinder. There, the potential is set equal to zero and the electric field is also zero so that eqs (15) hold. It is then quadrature to solve the Poisson-Boltzmann equation:

$$\Psi = 2 \ln \left(1 - \frac{1}{8} \bar{r}^2 \right) \quad (23)$$

The concentration $\bar{\rho}_i$ is determined from eqs (21) and (22).

$$\left(\frac{b}{\lambda} \right)^2 = \frac{8\pi\Lambda}{1 + \pi\Lambda} \quad (24)$$

$$\Lambda \equiv Q\sigma b$$

Hence, the osmotic pressure is conveniently expressed as

$$\begin{aligned} \pi_{os} &= \bar{\rho}_i k_B T \\ &= \frac{2\sigma k_B T}{b} \left(\frac{1}{1 + \pi\Lambda} \right) \end{aligned} \quad (25)$$

At small Λ , this reduces to a condition of electroneutrality as it should, since no counterions are condensed in this limit.

To progress, we need to set the variables σ and b . The size of the thin boundary layers discussed below is so small that they may be neglected in the following argumentation. The triangular region in fig 3 bears half an electron charge per length A along the major axis. The surface density of the effective cylinder is thus $\sigma = 1/4\pi bA$ implying that $\Lambda \simeq 2$ is independent of the interaxial spacing H ($Q/A = 4.2$ for DNA). The radius b is chosen such that the volumes of enclosed liquid are the same in the respective compartments.

$$\pi b^2 = \frac{1}{4} \sqrt{3} H^2 - \frac{1}{2} \pi a^2 \quad (26)$$

We rewrite eq (25) by introducing the volume fraction $v = \rho_0/\rho_{DNA}$ of DNA (the segment density of pure DNA = ρ_{DNA} ; the area of a hexagonal unit cell is $S = \sqrt{3}H^2/2$).

$$\begin{aligned} \pi_{os} &= \bar{\rho}_i k_B T \\ &= \frac{\rho_0 k_B T}{2(1 - v)} \end{aligned} \quad (27)$$

The density ρ_0 is identical to the uniform DNA density discussed in the previous section.

Obviously, our choice of cylinder parameters is not at all rigorous so the numerical coefficient in eq (27) is tentative. The scaling of parameters in eq (25) is convincing, however, because the correct limit given by eq (18) is attained at low densities ($H \gg a$ i.e. $\Lambda \gg 1$). Furthermore, the screening length λ is indeed small. For instance, at a separation h very close to zero, we have $b = 0.23a$ from eq (26) and since $\bar{\rho}_i \simeq 1/4\pi b^2 A$ we get $\lambda \simeq 0.47a$ from eq (24). Hence, the respective triangular sections (fig 3) in the entire lattice basically act as independent units as far as the electrostatics is concerned.

The thin boundary layers are treated in a Derjaguin approximation taking advantage of the relatively large radius ($a \gg \lambda$). Of course, discrete charge effects play a role now, so our analysis is not quantitatively accurate. For two flat plates of charge density $\sigma = 1/2\pi a A$ equal to that of DNA, we have

$$\pi_{os} = \frac{2\sigma k_B T}{h} \quad (28)$$

The scaled density $\Lambda_p \equiv \sigma Q h$, the analogue of Λ in eq (24), is much smaller than unity so the counterions are essentially uncondensed. The strategy of Derjaguin is to superpose normal forces exerted by opposing infinitesimal platelets on the two nearby charged objects (Israelachvili 1985). We therefore focus on two particular cylinders in fig 3 and introduce the plane defined by their centre axes. Two interacting platelets are located at a height x from this plane and the distance Z between them is $Z = h + 2z$ with $z = a - (a^2 - x^2)^{1/2}$. Hence, for relatively large a , we have $Z \simeq h + (x^2/a)$. The normal force between the two platelets per unit area is from eq (28)

$$\mathcal{F}_p(Z) = \frac{2\sigma k_B T}{Z} \quad (29)$$

and the total force between the two cylinders of length l is hence given by

$$\begin{aligned} \mathcal{F}(h) &\simeq 2l \int_{Z=h}^{\infty} dx \mathcal{F}_p(Z) \\ &= \frac{4\sigma l k_B T}{h} \int_0^{\infty} dx \left(1 + \frac{x^2}{ha}\right)^{-1} \\ &= 2\pi\sigma a^{1/2} h^{-1/2} l k_B T \end{aligned} \quad (30)$$

This can be integrated to give F_2 , the free energy of interaction between the two cylinders. If there are n rods in the actual hexagonal lattice, the total free energy is $F_{int} = 3nF_2$ for

there are six cylinders surrounding a test rod though we have to avoid doublecounting. By definition the osmotic pressure is

$$\begin{aligned}
\pi_{os,2} &= -\frac{1}{3^{1/2}nLH} \frac{\partial F_{int}}{\partial H} \\
&= \frac{3^{1/2}k_B T}{AHa^{1/2}h^{1/2}} \\
&= \frac{3H\rho_0 k_B T}{2a^{1/2}h^{1/2}} \tag{31}
\end{aligned}$$

upon using the density for DNA, $\sigma = 1/2\pi aA$ and eq (30).

At small separations the density $\bar{\rho}_i$ in the middle of the hollow cylinder (eq (27)) is the maximum density within the triangle in fig. 3. There is another $\bar{\rho}_{i,2}$ defined midway between the surfaces of two nearby cylinders. In accordance with eq (28), this is given by $\bar{\rho}_{i,2} \simeq 1/\pi ahA$ so the screening length $\lambda = Aha/4Q$ from eq (22) is quite small, significantly smaller, in fact, than the transverse scale $a^{1/2}h^{1/2}$ of the "surface of interaction" evident in the integrand of eq (30). This justifies the Derjaguin approximation but also the splitting up of the original triangular region into a hollow cylinder and three thin boundary layers. We now place the lattice in a reservoir containing monovalent electrolyte of concentration c_s . A Donnan equilibrium is established as described by eqs (16) and (17) with $\bar{\rho}_i$ given by eq (27).

4. Friction within condensed DNA

As the phage connector forces the DNA genome into a capsid, the DNA coil is bound to twist in view of its helical backbone. Since the other end probably also becomes constrained at some stage, we expect a twist-to-writhe transition to occur in dealing with the DNA dynamics. At first, the DNA density is statistically isotropic more or less, although the density decreases towards the central region owing to the curvature stress (Odijk & Slok 2003). As the concentration is enhanced, the excluded-volume effect, at some point, causes the DNA globule to become (probably) nematic in the outer confines of the capsid while the inner region remains isotropic (I disregard the chirality of the DNA interaction for simplicity). As more DNA is piled up into the phage, the entire globule could become nematic in a spoollike configuration. At the next stage, a hexagonal (or hexatic) phase

appears, again, in the outer region in coexistence with a nematic inner phase. Ultimately, at high degrees of packing, the entire structure becomes hexagonal apart from faults caused by frustration. This scenario is tentative of course. An a priori theory of globular organization is formidable as noted earlier. One problem is how the DNA loops are forced into ordered phases though we expect rippling transitions to occur (Odijk 1996).

I here present two highly simplified notions of the DNA dynamics. At low degrees of congestion, the usual reptation dynamics (de Gennes 1979) may be thought to apply, where a test chain slithers through a tubelike environment. Gabashvili and Grosberg (1992) already considered reptation during the ejection of DNA from phages. The friction the DNA experiences as it is transported through the connector, was also accounted for. Here, the reptation of DNA is discussed in the context of cyclization in order to gauge the accuracy of such a picture. At high degrees of congestion, the osmotic stress builds up because of the strong curvature stress. Simple reptation no longer seems likely then so I introduce a model based on sliding friction.

Cyclization within globules

The DNA is compacted into a globule by external forces (e.g. by adding inert polymer or multivalent ions, by confinement within a capsid in the initial stages). As argued by Ubbink and Odijk (1995, 1996), it is often possible to view the globular shape as being determined by balancing bending against surface forces while keeping the volume V_t fixed. For an ideal toroid defined by the two radii R_r and R_t shown in fig 4, the surface area is $A_t = 4\pi^2 R_r R_t$ and the volume $V_t = SL = 2\pi^2 R_r^2 R_t$ is also given in terms of the (constant) area S of the unit cell. The two ends would never come into contact if the shape of the toroid were to remain the same, for the free energy of change in volume is prohibitive. We thus investigate fluctuations in the globular shape. I disregard free energy contributions arising from crossovers, knots and other defects (Park et al 1998; Arsuaga et al 2002; Hud & Downing 2001; Nelson 2002).

The curvature stress is low if $R_t \gtrsim 2R_r$ (Ubbink & Odijk 1995; Ubbink & Odijk 1996). Under these conditions the bending energy (eq (1)) is approximated by

$$U \simeq \frac{PL}{2R_t^2} \quad (32)$$

There is a surface tension σ scaled by $k_B T$ whatever the mechanism of compaction. The

surface free energy is then

$$F_S = \sigma A_t k_B T \quad (33)$$

Since V_t is constrained, we eliminate one of the radii so as to express the total free energy in units of $k_B T$ as

$$F_t = \frac{1}{2} P L R_t^{-2} + 2^{3/2} \pi \sigma R_t^{1/2} V_t^{1/2} \quad (34)$$

Minimization of F_t with respect to R_t yields an optimum radius of the toroid

$$R_{t,m}^{5/2} = \frac{P L}{2^{1/2} \pi \sigma V_t^{1/2}} \quad (35)$$

Therefore, the fluctuations in globular shape are governed by a Gaussian distribution

$$G \propto \exp -\frac{1}{2} F_t'' \Delta R_t^2 \quad (36)$$

$$\langle \Delta R_t^2 \rangle \equiv \langle (R_t - R_{t,m})^2 \rangle = (F_t'')^{-1}$$

$$F_t'' = \frac{5}{2} P L R_{t,m}^{-4}$$

This is derived by a straightforward Taylor expansion of eq (34) within the Boltzmann factor $\exp(-F_t)$.

We next need to assess how the winding number n changes in response to alterations in shape. This is simply $nS = \pi R_r^2$ so a fluctuation in n is given by $\delta n = 2\pi R_{r,m} \delta R_r / S$. The volume constraint implies $2R_{r,m} R_{t,m} \delta R_c + R_{r,m}^2 \delta R_t = 0$. If the two ends are to meet, we require $\delta n \geq 1$, leading to an inequality for the second moment (via eq (36)). We finally attain the condition $L > 10\pi^2 P$ which, remarkably, is independent of the surface tension. Accordingly, by this mechanism, cyclization can only occur if the DNA is quite long.

A reptation time for cyclization is now readily written down by dimensional reasoning. It must be proportional to the friction exerted by the fluid (water presumably, with a viscosity η_0 , since the globule is not very compact), i.e. proportional to the contour length L . For cyclization, one of the DNA ends has to diffuse a distance, typically about πR_t at least, with respect to the other end.

$$\tau_r \simeq \frac{(\pi R_t)^2 L \eta_0}{k_B T} \quad (37)$$

We do not address the dynamics of the two ends as they approach each other within a region of size $\sim R_r$.

Sliding friction in highly compacted states

Let us first consider a classic example of Coulomb friction (Persson 2000). A block of some material rests on a flat surface (fig 5). Owing to gravity, for instance, the block exerts a pressure \mathcal{F}_s/Ω on a section of the surface of area Ω . If we now exert a force \mathcal{F}_t on the block, tangential to the surface, the blocks fails to move at first. It is only at a certain \mathcal{F}_t given by

$$\frac{\mathcal{F}_t}{\mathcal{F}_s} = \frac{\mathcal{F}_t/\Omega}{\mathcal{F}_s/\Omega} = \omega \quad (38)$$

that the block is set in motion. The friction constant ω is well defined, at least within certain bounds on the velocity thus induced.

In a highly congested DNA globule compressed by bending stresses, we may also discern a pressure π_{os} acting on a surface area $2\sqrt{3}LH$ where $2\sqrt{3}H$ is the length of the perimeter of the unit cell assumed to be hexagonal. Hence, the minimum force needed to set the DNA in motion should be

$$\begin{aligned} \mathcal{F}_t &= 2\sqrt{3}\omega HL\pi_{os} \\ &\simeq \frac{2\omega LPk_B T}{HE_i^2} \end{aligned} \quad (39)$$

At very high degrees of packing, the first term in eq (12) may be neglected. The minimum force increases fast upon further packaging of DNA in a phage (increasing L , decreasing H and E_i). It has been assumed that the DNA slides homogeneously through its own tubelike environment.

5. Discussion

Ordered phases in the bulk and in phages

It is important to summarize several results for liquid-crystalline DNA in the bulk that are relevant to DNA packaged within phages. The literature on DNA liquid crystals in vitro is vast and has been reviewed elsewhere (Livolant & Leforestier 1996). Durand et al (1992) performed careful X-ray diffraction experiments on slowly evaporating suspensions of 50 nm long DNA rods. The sequence of phase transitions was argued to be: isotropic - cholesteric - 2d hexagonal - 3d hexagonal - orthorhombic. The transitions are first order except for the one between the two hexagonal phases. In the 2d hexagonal phase, the rods are free

to move longitudinally but this freedom is gradually frozen out as the DNA concentration increases, so the 2d-3d transition is continuous. The solution only becomes orthorhombic at a very high concentration of 670 g/l (the interaxial spacing $H = 2.37$ nm in the coexisting 3d hexagonal phase). The helical repeat actually decreases quite dramatically from 3.5 nm to 3.0 nm within the sequence of positionally ordered phases, whereas the B conformation remains surprisingly intact with a constant rise $= 2A = 0.336$ nm. The buffer contained 0.25 M electrolyte (either ammonium acetate or sodium chloride) so these data are pertinent to the packing of DNA under physiological conditions.

The ionic-strength dependence of the cholesteric-hexagonal transition for DNA of length almost 50 nm was monitored by Kassapidou et al (1998), the hexagonal spacings at coexistence ranging from 3.7 nm at 0.10 M NaCl to 3.0 nm at 1.65 M. The orientational fluctuations measured by neutron scattering were close to 10 degrees. The first-order transition is visible, in fact, in a test tube with a clear meniscus discernible between the two phases and the hexagonal phase exhibits the characteristic fanlike texture under a polarizing microscope (J.R.C. van der Maarel, private communication, 1998).

On the other hand, Strey et al (2000) do not seem to witness the X-ray diffraction characteristic of hexagonal order, for concentrated Calf-Thymus DNA in 0.5 M NaCl, that has been wet-spun. One potential drawback is that the long DNA is quite polydisperse which could prevent a phase transition applicable to very long monodisperse DNA. Anyway, the azimuthal scattering has sixfold symmetry so that the phase is probably hexatic. If so, the decay in the orientational order should be algebraic (Nelson 2002) with an exponent depending on the conditions (like the ionic strength). This ought to be gleaned from the scattering curves (Lyuksyutov et al 1992).

Spool models have been adopted as models of DNA packaged in bacteriophages (Harrison 1973). X-ray diffraction patterns from phages have often been interpreted in terms of hexagonal packing of the DNA (North & Rich 1961; Earnshaw & Harrison 1977; Stroud et al 1981; Rontó et al 1988; Booy et al 1991; Cerritelli et al 1997; Bhella et al 2000). Cerritelli et al (1997) have adduced quite convincing evidence for the validity of the spool form for well-aligned bacteriophage T7. Earnshaw and Harrison (1977) pointed out that the inner region of the DNA spool should be more disordered. A theory of the nonuniform density of the DNA inside phages was set up recently (Odijk & Slok 2003) in which a cholesteric-hexagonal transition could be exhibited even under conditions of rather tight packing (note

the spacings quoted above). Physicists have analyzed the X-ray scattering by nematic liquid crystals of poly- γ -benzyl glutamate in terms of density fluctuations (Ao et al 1991). These are coupled to director fluctuations by so-called continuity laws (de Gennes 1977, Selinger & Bruinsma 1991, Kamien et al 1992). The intensity spectrum as a function of the scattering vector has a characteristic bowtie shape. There is a typical length scale associated with these fluctuations which is determined by a trade-off of bending versus osmotic compressibility (de Gennes 1977). This turns out to be similar in size to E_i the radius of the inner hole of the spool inside phages (bulk hexagonal DNA here being compared to phage DNA). Thus, it would be of some interest to reinvestigate the scattering by the inner region of the DNA spool from this point of view (Odijk & Slok 2003).

The osmotic pressure of DNA solutions has also been readdressed recently (Strey et al 1999, Raspaud et al 2000). At very high concentrations where the phase is hexagonal or hexatic (but I shall assume it to be hexagonal for definiteness), there are significant deviations from the Oosawa theory (eqs (17) and (18)). The approximate theory in terms of a hollow cylinder and thin boundary layers goes some way towards explaining the high values of π_{os} (Strey et al 1999). For instance, at a DNA concentration of 1.2 monoM, eq (27) predicts 2.4×10^6 N/m² in good agreement with experiment (eq (31) does not apply since the separation is $h = \mathcal{O}(a)$ and not $h \ll a$). At a concentration of 1.8 monoM, eqs (27) and (31) yield osmotic pressures 5.2×10^6 N/m² and 13×10^6 N/m² respectively, compared with the experimental 13×10^6 N/m² (Strey et al 1999).

Till now, we have neglected configurational entropy. The free energy of a wormlike chain trapped in a tube of diameter less than the persistence length P was formulated long ago (Odijk 1983) and has been discussed many times since. For DNA confined within a hexagonal lattice, we may write on the basis of scaling arguments (Odijk 1983, Selinger & Bruinsma 1991)

$$f_{en}(S) = \frac{c_1}{h^{2/3} P^{1/3}} \quad (40)$$

$$\pi_{os} = \frac{2c_1}{3^{3/2} h^{5/3} H P^{1/3}} \quad (41)$$

Unfortunately, the coefficient c_1 is not at all known accurately for a hexagonal phase. Setting the coefficient $c_1 = 1$ and using eqs (7), (12) and (14) lead to a semiquantitative explanation of the fairly sharp rise in the loading force as an elastic worm becomes densely packed in a cavity (see the simulations of Kindt et al (2001) and of Marenduzzo and Micheletti

(2003). The latter authors also find that there is a section of chain aligned within the cylindrical hole of the spool. Arsuaga et al (2002) put forward evidence for an inner region misaligned with the well-ordered outer spool under conditions of intermediate packaging but the effects of realistic electrostatics on these computations need to be awaited.) For comparison, the osmotic pressure of the entropic interaction is $5.3 \times 10^5 \text{ N/m}^2$ at 1.8 monoM, an order of magnitude smaller than the pressures quoted above ($h = 0.51 \text{ nm}$, $P = 50 \text{ nm}$). Nevertheless, the nonlinear coupling between electrostatics and undulatory entropy probably needs looking into (see the work of De Vries (1997) on undulating charged surfaces in the salt-free Poisson-Boltzmann approximation).

Loading forces and inner radii

At high degrees of packing, the terms containing U in eqs (12), (13) and (14) are negligible so the relevant thermodynamic parameters reduce to $\mathcal{P} \simeq \pi_{os} \simeq Pk_B T/2SE^2$ and $|\mathcal{F}| = f + S\pi_{os}$. The hole inside a spoollike region may have caps belonging to the wall of the capsid, a fact disregarded in section 2, but this effect gives only corrections of $\mathcal{O}(E_i^2/V_0^{2/3})$. We thus regain eq (10) of Odijk (1998) valid for a specific model, which itself is in good agreement with the DNA spacings measured inside bacteriophage T7 by Cerritelli et al (1997), Odijk (1998) employed the simple Oosawa model (eqs (17) and (18)). In recent papers, Tzlil et al (2002) and Purohit et al (2003) have used a different form: $\pi_{os} = \pi_0[\exp(H_0 - H)/\lambda_H - 1]$ with $\pi_0 = 0.12 k_B T/\text{nm}^3$, decay length $\lambda_H = 0.14 \text{ nm}$ and $H_0 = 2.8 \text{ nm}$ stemming from the osmotic stress measurements of Rau & Parsegian (1992) on DNA greatly perturbed by trivalent cobalt hexammine ions. Why this interaction, attractive in part, should generally prevail inside phages is not clear. Anyway, the spacings predicted by eqs (7) and (12) upon inserting this form, are virtually identical to those in table 1 of Tzlil et al (2002). The inner radius E_i is now 2.81 nm when the entire genome is packaged.

The supposition of uniform density has been released in a recent analysis based on eq. (3) (Odijk & Slok 2003). In a density functional approach, the gradient terms are small because they exert themselves on a scale λ or H only. The curvature stress is balanced against the chemical potential of inhomogeneous bulk DNA. The hole size is given by an expression similar to eq (12) but the tightly wound region surrounding the hole has an inhomogeneous density varying on a scale E_i (Odijk & Slok 2003). Such a profile seems to be in qualitative agreement with experiments of Olson et al (2001) on the T4 phage.

The forces of encapsidation have been monitored in single-molecule experiments by Smith et al (2001). I shall try to interpret this force semiempirically. It seems a good Ansatz to set the osmotic pressure $\pi_{os}/k_B T = \bar{\rho}_i = c_2 \rho_0 = c_2/AS$ within a certain interval of the DNA concentration in the absence of salt (see eqs (27) and (31) here, and fig 2 of Hansen et al (2001)). We then need the quantity $f(S)$ at a certain ionic strength of the buffer. There is a Donnan equilibrium given by eq (17) and the free energy has been computed by Odijk & Slok (2003). We therefore obtain for the force $|\mathcal{F}| = f(S) + S\pi_{os} = (c_2 k_B T/A)[1 - \ln w]$ with $w = 2c_s/\bar{\rho}_i = 2ASc_s/c_2 \ll 1$. Smith et al (2001) measured a maximum loading force of 50 pN at a buffer concentration c_s of about 0.1 M. The inner volume of the phi29 capsid can be approximated by an ellipsoid of major axis equal to 25.5 nm and minor axis equal to 19.5 nm (Tao et al 1998; P.J. Jardine, private communication, 2000). Hence we have $V_0 = 40600 \text{ nm}^3$ and so the unit cell has dimensions $S \simeq 6.2 \text{ nm}^2$ and $H \simeq 2.7 \text{ nm}$ for a genome length L_{max} if we disregard the very small inner hole of size $E_i = 2.4 \text{ nm}$, computed from eq (12) upon a first iteration. We finally calculate $c_2 = 0.73$ and the osmotic pressure π_{os} is about 29 atm. This underestimates the theoretical and experimental bulk pressures a bit but the effect of magnesium ions in the force set-up has not been accounted for.

However, there are difficulties in the interpretation of the force-length curve below the limit of full packing. If the inner hole remains fairly small, we may express the derivative as

$$\frac{\partial|\mathcal{F}|}{\partial L} \simeq -\frac{S^2}{L} \frac{\partial\pi_{os}}{\partial S} \quad (42)$$

using eqs (7) and (14). Accordingly, $\partial|\mathcal{F}|/\partial L = c_2 k_B T/AL = 18 \text{ pN per } L_{max}$ if $\pi_{os} = c_1 \rho_0$. This is not unreasonable if $L \simeq L_{max}$ (see Smith et al 2001) but fails utterly when $0.4 < L/L_{max} < 0.9$, for $\partial|\mathcal{F}|/\partial L$ increases upon compaction in that case. It appears that we must have the osmotic pressure increasing as ρ_0^2 at least. What could be the cause of such a high effective power, granting that the measured force does not reflect dissipative losses? First, the crossover concentration demarcating the validity of the Oosawa model vis-à-vis a model with complete hexagonal detail is about 0.8 monoM judging from fig 2 of Hansen et al (2001) ($L = 0.5L_{max}$ at this concentration). Thus, counterions are gradually decondensing within the anomalous range of contour lengths. In addition, the Donnan effect is also slowly diminishing and the effect of the thin boundary layers is also becoming appreciable. An increase of the pressure stronger than linear is not surprising though this issue merits further quantitative study. (Parenthetically, a problem possibly related to this

could be the curvature in the rate-length curves determined by P.J. Jardine, opposite to the one measured by Smith et al (2001) (P.J. Jardine, private communications, 2000, 2001). He packaged DNA in phi29 phages in vitro by adding ATP to the solution. The reaction was effectively blocked with the help of gamma-S-ATP and the length of DNA injected was quantified as a function of time using a restriction enzyme.)

The inner radii computed above at a high degree of packing are very small. An important problem that now arises is whether such tiny radii are viable, both physically and biologically. We are here concerned with the tight curvature of long sections of solenoidal DNA independent of the base pair sequence and in the absence of bound proteins. Crick and Klug (1975) already quoted values of 3 to 5 nm for radii of curvature that could pose potential problems with regard to smooth bending. Sussman & Trifonov (1978) estimated a critical radius of kinking of about 2.5 nm by equating the elastic bending energy to the maximum enthalpy of stacking the base pairs assuming one kink per helical repeat. A more detailed treatment based on Van der Waals contacts led to a minimum acceptable radius of about 5 nm. More recently, a 51 bp microcircle with a radius of curvature of 2.8 nm was devised by exploiting current computer modelling techniques (Tung & Soumpasis 1995). 42 bp microcircles have actually been constructed in the laboratory (Wolters & Wittig 1989, 1990) but the base pair sequence is from a promotor. On the whole, a viable minimum radius would thus seem to be 3 nm or only very slightly smaller (A. Travers, private communication, 2003). The inner radii E_i within phages that we have computed above are dangerously small. It is possible that the energy of curvature becomes anharmonic at small radii which would increase estimates of E_i somewhat. Any kinking would, of course, render invalid the models outlined here.

DNA self-friction

Jary and Sikorav (1999) investigated the monomolecular collapse of lambda DNA caused by the trivalent polyamine spermidine and the attendant rate of cyclization of the DNA. Fortunately, the collapse is very fast so it is possible to monitor the cyclization in the toroidal globular state quite accurately. The measured rates were between about 1 to 10 s^{-1} . This compares favourably with the reptation time from eq (37) (the viscosity of water $\eta_0 = 1$ cP at room temperature, the contour length $L = 17 \mu\text{m}$ and $R_t \simeq 60$ nm (Widom & Baldwin 1983)). We conclude that the DNA apparently experiences friction from the "water" alone,

despite the fact that the typical spacing in such a globule is small ($H \simeq 2.8$ nm).

In a tightly packed phage, the dynamics of the DNA could be markedly different from that in globules, because of the much higher bending stress. In evaluating the frictional forces between two surfaces separated by a very thin layer of intervening fluid, one introduces a dimensionless group, $\eta_0 u / \pi_{os}$ in this case, where \vec{u} is the velocity tangential to the surface (see fig 5; Persson 2000). In DNA encapsidation within a phage, this velocity is so small (Smith et al 2001), that this quantity is minute so we ought to have boundary lubrication rather than hydrodynamic lubrication. The friction coefficient ω would be about 10^{-1} (Persson 2000). In principle, there should then be a tendency for the water to be squeezed out between two adjacent DNA strands. Because there are only a few water molecules between the strands, layering transitions would be possible (Zilberman et al 2001) depending on the degree of commensurability of the two DNA backbones (Müser et al 2001). However, eq (39) would now predict a minimum force more than 100 times larger than the 50 pN force observed in the phi29 phage. A possible resolution of this paradox is the very recent assessment of sliding friction between surfaces with intervening aqueous nanolayers (Raviv et al 2001, Raviv & Klein 2002). Surprisingly, the water still acts almost like a hydrodynamic bulk fluid, possibly because the hydrogen bonds are suppressed under conditions of sliding nanofriction. The friction coefficient could now be as low as 10^{-3} so the 50 pN force (Smith et al 2001) may be just enough to overcome the minimum force. It is also remarked that the free energy of compacting DNA into the phi29 phage is about $1 k_B T$ per bp (Smith et al 2001) to be compared with the enthalpy of expulsion, $0.80 k_B T$ per bp, measured by calorimetry for bacteriophage T7 (Raman et al 2001; Serwer 2003), though the packing conditions in these two phages are not identical. Obviously, the problem of dissipative losses, if any, merits further attention.

6. Concluding Remarks

Clearly, our understanding of DNA packing in bacteriophages is incomplete. Although we may rationalize the high osmotic pressures and loading forces as being caused by the small separation between DNA helices, the tight inner radii of the spools are too close to kinking for comfort. At intermediate degrees of packing, we lack a precise theory of the electrostatic interaction in terms of the fraction of counterions condensed on the DNA. The

loading forces are very sensitive to detail in the interaction in this regime. An open problem is the friction at a high degree of compaction and its nature - is it hydrodynamic lubrication? Lastly, magnesium ions are often present in the buffers used. Their impact on the Donnan equilibrium needs to be investigated.

Acknowledgment

I am grateful to Jean-Louis Sikorav, Edouard Yeramian and Paul Jardine for discussions, and the latter for extended correspondence on phages and packaging. Professor Andrew Travers is thanked for very helpful thoughts on the minimum radius of curvature of DNA. The insights of Flodder Slok proved most welcome.

references

- Ao, X., Wen, X. & Meyer, R.B. 1991 X-ray scattering from polymer nematic liquid crystals. *Physica A* **176**, 63-71.
- Arsuaga, J., Vázquez, M., Trigueros, S., De Witt Sumners & Roca, J. 2002 Knotting probability of DNA molecules confined in restricted volumes: DNA knotting in phage capsids. *Proc. Natl. Acad. Sci. U.S.A.* **99**, 5373-5377.
- Arsuaga, J., Tan R.K.Z., Vázquez, M., De Witt Sumners & Harvey, S.C. 2002 Investigation of viral DNA packaging using molecular mechanics models. *Biophys. Chem.* **101-102**, 475-484.
- Bhella, D., Rixon, F.J. & Dargan, D.J. 2000 Cryomicroscopy of human cytomegalovirus virions reveals more densely packed genomic DNA than in herpes simplex virus type 1. *J. Mol. Biol.* **295**, 155-161.
- Booy, F.P., Newcomb, W.W., Trus, B.L., Brown, J.C., Baker, T.S. & Steven, A.C. 1991 Liquid crystalline, phage-like packing of encapsidated DNA in herpes simplex virus. *Cell* **64**, 1007-1015.
- Cerritelli, M.E., Cheng, N., Rosenberg, A.H., McPherson, C.E., Booy, F.P. & Steven, A.C. 1997 Encapsidated conformation of bacteriophage T7 DNA. *Cell* **91**, 271-280.
- Crick, F.H.C. & Klug, A. 1975 Kinky helix. *Nature* **255**, 530-533.
- de Gennes, P.G. 1977 Polymeric liquid crystals: Frank elasticity and light scattering. *Mol. Cryst. Liq. Cryst.* **34**, 177-182.
- de Gennes, P.G. 1979 *Scaling concepts in polymer physics*. Cornell University Press, Ithaca, N.Y.
- de Vries, R. 1997 Thermal undulations in salt-free charged lamellar phases: theory versus experiment. *Phys. Rev. E* **56**, 1879-1886.
- Durand, D., Doucet, J. & Livolant, F. 1992 A study of the structure of highly concentrated phases of DNA by X-ray diffraction. *J. Phys. II France* **2** **9**, 1769-1783.

- Earnshaw, W.C. & Harrison, S.C. 1977 DNA arrangement in isometric phage heads. *Nature* **268**, 598-602.
- Fixman, M. 1979 The Poisson-Boltzmann equation and its application to polyelectrolytes. *J. Chem. Phys.* **70**, 4995-5005.
- Gabashvili, I.S., Grosberg, A.Yu., Kuznetsov, D.V. & Mrevlishvili, G.M. 1991 Theoretical model of DNA packing in the phage head. *Biophysics* **36**, 782-789
- Gabashvili, I.S. & Grosberg, A.Yu. 1992 Dynamics of double stranded DNA reptation from bacteriophage. *J. Biomol. Struct. Dyn.* **9**, 911-920.
- Grimes, S., Anderson, D.L., Baker, T.S. & Rossmann, M.G. 2000 Structure of the bacteriophage phi29 DNA packaging motor. *Nature* **408**, 745-750.
- Grimes, S., Jardine, P.J. & Anderson, D. 2002 Bacteriophage phi29 DNA packaging. *Adv. Vir. Res.* **58**, 255-294.
- Hansen, P.L., Podgornik, R. & Parsegian, V.A. 2001 Osmotic properties of DNA: critical evaluation of counterion condensation theory. *Phys. Rev. E* **64**, 021907 (1-4).
- Harrison, S.C. 1983 Packaging of DNA into bacteriophage heads: A model. *J. Mol. Biol.* **171**, 577-580
- Hud, N.V. & Downing, K.H. 2001 Cryoelectron microscopy of lambda phage DNA condensates in vitreous ice: The fine structure of DNA toroids. *Proc. Natl. Acad. Sci. USA* **98**, 14925-14931.
- Israelachvili, J.N. 1985 *Intermolecular and surface forces*, Academic, London.
- Jardine, P.J. & Anderson, D. 2003 DNA packaging. In *The Bacteriophages*, Ed. R. Calendar, Oxford University Press, in press.
- Jary, D. & Sikorav, J.-L. 1999 Cyclization of globular DNA. Implications for DNA-DNA interactions in vivo. *Biochemistry* **38**, 3223-3227.
- Kamien, R.D., Le Doussal, P. & Nelson, D.R. 1992 Theory of directed polymers. *Phys. Rev. A* **45**, 8727-8750.

- Kassapidou, K. & Van der Maarel, J.R.C. 1998 Melting of columnar hexagonal DNA liquid crystals. *Eur. Phys. J. B.* **3**, 471-476.
- Kindt, J., Tzilil, A., Ben-Shaul, A. & Gelbart, W.M. 2001 DNA packaging and ejection forces in bacteriophage. *Proc. Natl. Acad. Sci. USA* **98**, 13671-13674.
- Livolant, F. & Leforestier, A. 1996 Condensed phases of DNA: structure and phase transitions. *Prog. Polym. Sci.* **21**, 1115-1164.
- Lyuksyutov I., Naumovets, A.G. & Pokrovsky, V. 1992 *Two-dimensional crystals Academic*, San Diego, CA.
- Manning, G.S. 1969 Limiting laws and counterion condensation in polyelectrolyte solutions. I. Colligative properties. *J. Chem. Phys.* **51**, 924-933
- Marenduzzo, D. & Micheletti, C. 2003 Thermodynamics of DNA packaging inside a viral capsid: the role of DNA intrinsic thickness, preprint.
- Müser, M.H., Wenning, L. & Robbins, M.O. 2001 Simple microscopic theory of Amontons's laws for static friction. *Phys. Rev. Lett.* **86**, 1295-1298.
- Nelson, D.R. 2002 *Defects and geometry in condensed matter physics*. Cambridge University Press, U.K.
- North, A.C.T. & Rich, A. 1961 X-ray diffraction studies of bacterial viruses. *Nature* **191**, 1242-1247.
- Odijk, T. 1983 On the statistics and dynamics of confined or entangled stiff polymers. *Macromolecules* **16**, 1340-1344.
- Odijk, T. 1986 Elastic constants of nematic solutions of rodlike and semiflexible polymers. *Liquid Crystals* **1**, 553-559.
- Odijk, T. 1996 DNA in a liquid-crystalline environment: tight bends, rings, supercoils. *J. Chem. Phys.* **105**, 1270-1286.
- Odijk, T. 1998 Hexagonally packed DNA within bacteriophage T7 stabilized by curvature stress. *Biophys.J.* **75**, 1223-1227.

- Odijk, T. & Slok, F. 2003 Nonuniform Donnan equilibrium within bacteriophages packed with DNA. *J. Phys. Chem. B.* in press.
- Olson, N.H., Gingery, M., Eiserling, F.A. & Baker, T.S. 2001 The structure of isometric capsids of bacteriophage T4. *Virology* **279**, 385-391.
- Oosawa, F. 1971 *Polyelectrolytes*, Marcel Dekker, New York.
- Park, S.Y., Harries, D. & Gelbart, W.M. 1998 Topological defects and the optimum size of DNA condensates. *Biophys. J.* **75**, 714-720.
- Pereira, G.G. & Williams, D.R.M. 2000 Crystalline toroidal globules of DNA and other semiflexible polymers: jumps in radius caused by hexagonal packing. *Europhys. Lett.* **50**, 559-564.
- Persson, B.N.J. 2000 *Sliding friction*. Springer, Berlin, 2nd ed.
- Purohit, P.K., Kondev, J. & Phillips, R. 2003 Mechanics of DNA packaging in viruses. *Proc. Natl. Acad. Sci. USA* **100**, 3173-3178.
- Raman, C.S., Hayes, S.J., Nall, B.T. & Serwer, P. 2001 Energy stored in the packaged DNA of bacteriophage T7. *Biophys. J.* **65**, A12.
- Raspaud, E., Da Conceição, M. & Livolant, F. 2000 Do free DNA counterions control the osmotic pressure? *Phys. Rev. Lett.* **84**, 2533-2536.
- Rau, D.C. & Parsegian, V.A. 1992 Direct measurement of the intermolecular forces between counterion-condensed DNA double helices. *Biophys. J.* **61**, 246-259.
- Raviv, U., Laurat, P. & Klein, J. 2001 Fluidity of water confined to subnanometre films. *Nature* **413**, 51-54.
- Raviv, U. & Klein, J. 2002 Fluidity of bound hydration layers. *Science* **297**, 1540-1543.
- Reimer, S.C. & Bloomfield, V.A. 1978 Packaging of DNA in bacteriophage heads: some considerations on energetics. *Biopolymers* **17**, 785-794.
- Rontó, Gy., Tóth, K., Feigin, L.A., Svergun, D.I. & Dembo, A.T. 1988 Symmetry and structure of bacteriophage T7. *Comput. Math. Applic.* **16**, 617-628.

- Selinger, J.V. & Bruinsma, R.F. 1991 Hexagonal and nematic phases of chains. I. Correlation functions. *Phys. Rev. A* **43**, 2910-2921.
- Serwer, P. 2003 Models of bacteriophage DNA packaging motors. *J. Struct. Biol.* **141**, 179-188.
- Simpson, A.A., Tao, Y., Leiman, P.G., Badasso, M.O., He Y., Jardine, P.J., Olson, N.H., Morals, M.C., Grimes, S., Anderson, D.L., Baker, T.S. & Rossmann, M.G. 2000 Structure of the bacteriophage phi29 DNA packaging motor. *Nature* **408**, 745-750.
- Smith, D.E. Tans, S.J., Smith, S.B., Grimes, S., Anderson, D.L. & Bustamante, C. The bacteriophage phi29 portal motor can package DNA against a large internal force. *Nature* **413**, 748-752.
- Strey, H.H., Parsegian, V.A. & Podgornik, R. 1999 Equation of state for polymer liquid crystals: Theory and experiment. *Phys. Rev. E* **59**, 999-1008.
- Strey, H.H., Wang, J., Podgornik, R., Rupprecht, A., Yu, L., Parsegian, V.A. & Sitora, E.B. 2000 Refusing to twist: Demonstration of a line hexatic phase in DNA liquid crystals. *Phys. Rev. Lett.* **84**, 3105-3108.
- Stroud, R.M., Serwer, P. & Ross, M.J. 1981 Assembly of bacteriophage T7. Dimensions of the bacteriophage and its capsids. *Biophys. J.* **36**, 743-757.
- Sussman, J.L. & Trifonov, E.N. 1978 Possibility of nonkinked packing of DNA in chromatin. *Proc. Natl. Acad. Sci. USA* **75**, 103-107.
- Tao, Y., Olson, N.H., Xu, W., Anderson, D.L., Rossmann, M.G. & Baker, T.S. 1998 Assembly of a tailed bacterial virus and its genome release studied in three dimensions. *Cell* **95**, 431-437.
- Tung, C.S. & Soumpasis, D.M. 1995 The construction of DNA helical duplexes along prescribed 3-D curves. *J. Biomol. Struct. Dyn.* **13**, 577-582.
- Tzlil, S., Kindt, J.T. Gelbart, W.M. & Ben-Shaul, A. 2003 Forces and pressures in DNA packaging and release from viral capsids. *Biophys. J.* **84**, 1616-1627.

- Ubbink, J. & Odijk, T. 1995 Polymer- and salt-induced toroids of hexagonal DNA. *Biophys. J.* **68**, 54-61.
- Ubbink, J. & Odijk, T. 1996 Deformation of toroidal DNA condensates under surface stress. *Europhys. Lett.* **33**, 353-358.
- Widom, J. & Baldwin, R.L. 1983 Monomolecular condensation of lambda-DNA induced by cobalt hexammine. *Biopolymers* **22**, 1595-1620.
- Wolters, M. & Wittig, B. 1989. Construction of a 42 base pair double stranded DNA microcircle. *Nucl. Acids Res.* **17**, 5163-5172.
- Wolters, M. & Wittig, B. 1990. A strategy for the construction of double-stranded DNA microcircles with circumferences less than 50 bp. *Anti-Cancer Drug Design* **5**, 111-120.
- Yamakawa, H. 1971 *Modern theory of polymer solutions*. Harper & Row, New York.
- Zilberman, S., Persson, B.N.J., Nitzan, A., Mugele, F. & Salmeron, M. 2001 Boundary lubrication: dynamics of squeeze-out. *Phys. Rev. E* **63**, 055103 (R) (1-4).

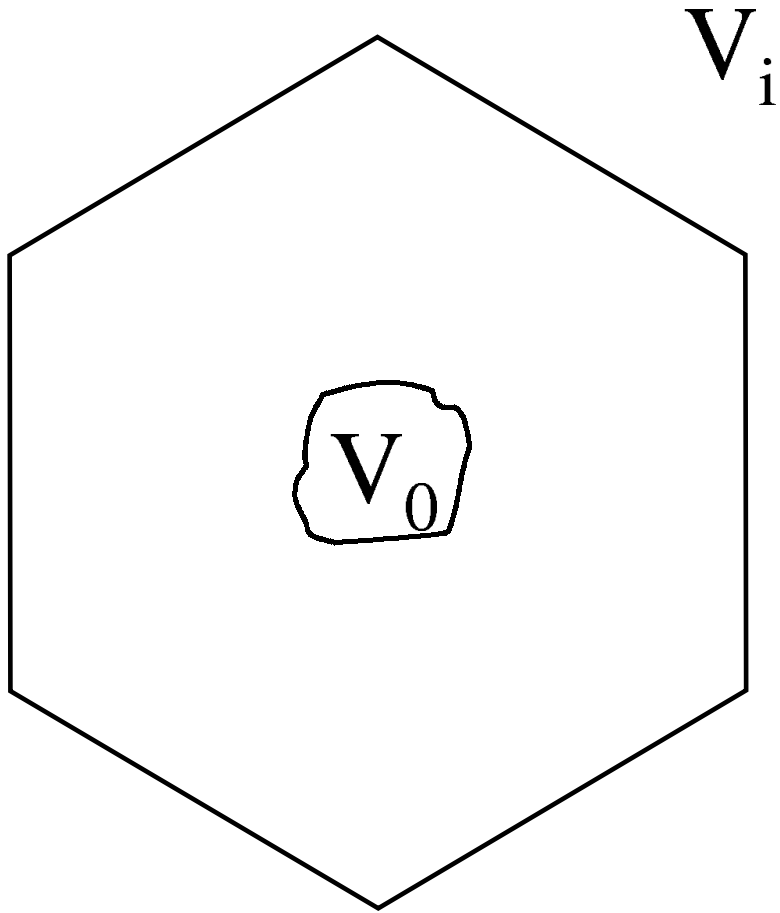


FIG. 1: A capsid packed with DNA down to an inner hole of volume V_0 .

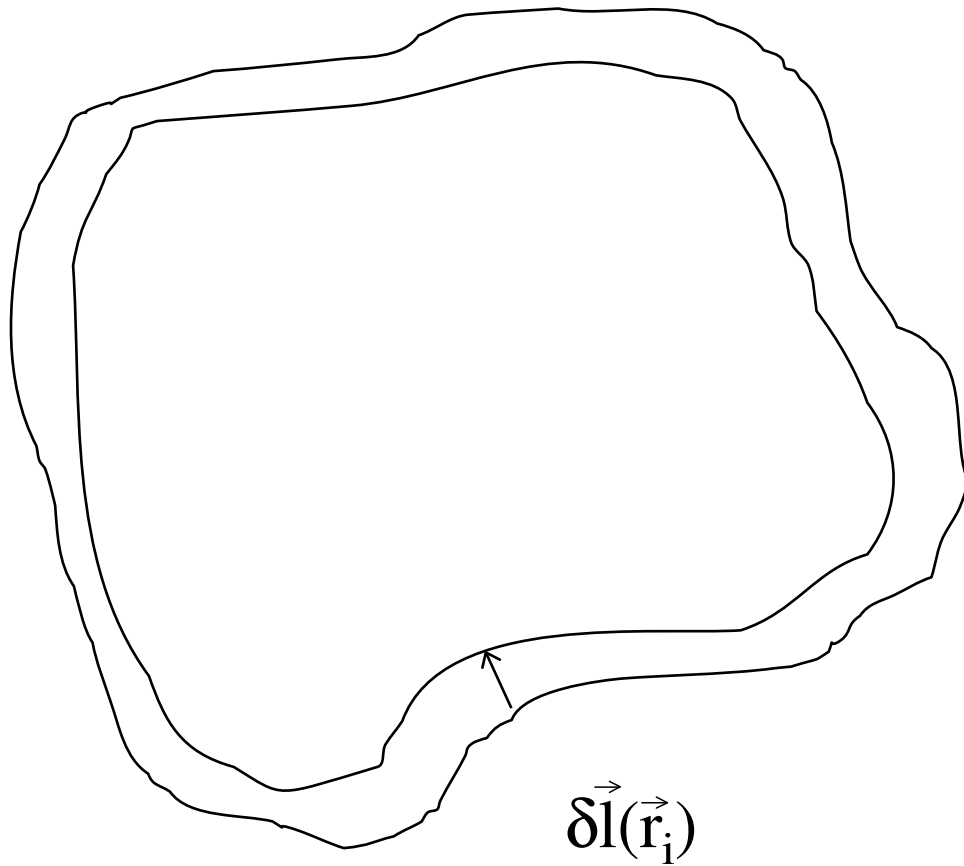


FIG. 2: The variational decrease in the size of the hole within the DNA spool.

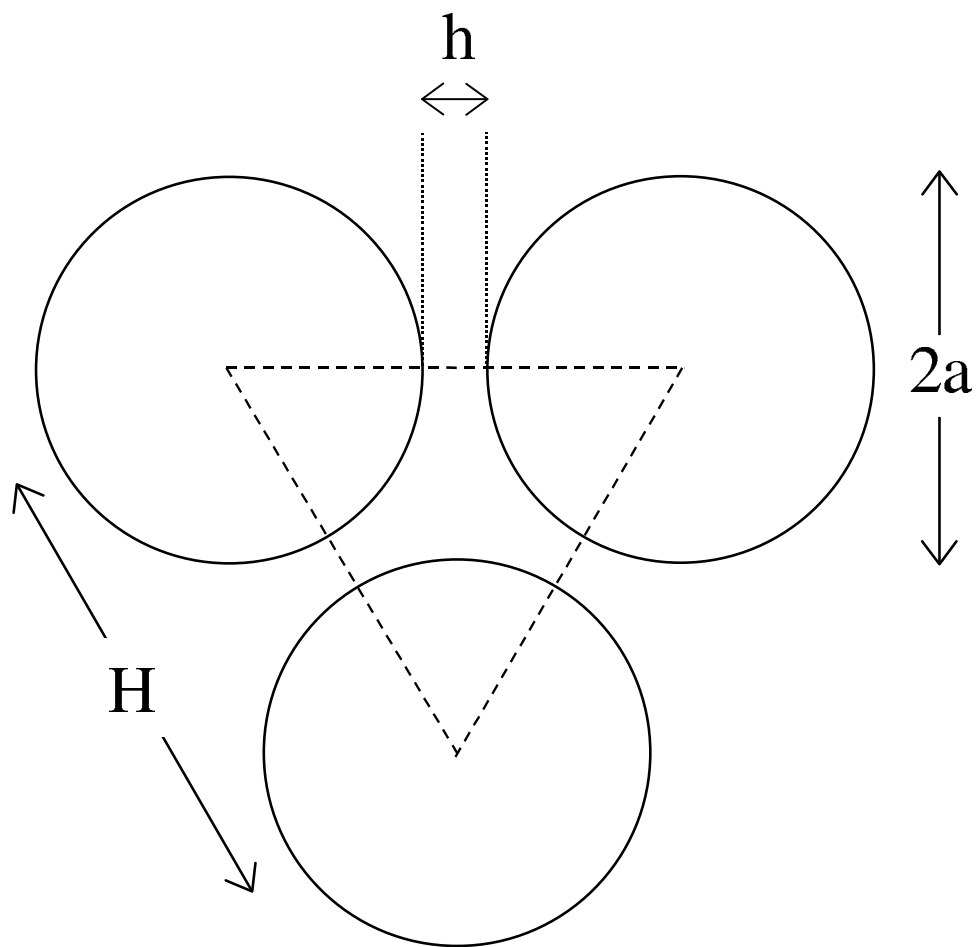


FIG. 3: Three DNA cylinders within the hexagonal lattice.

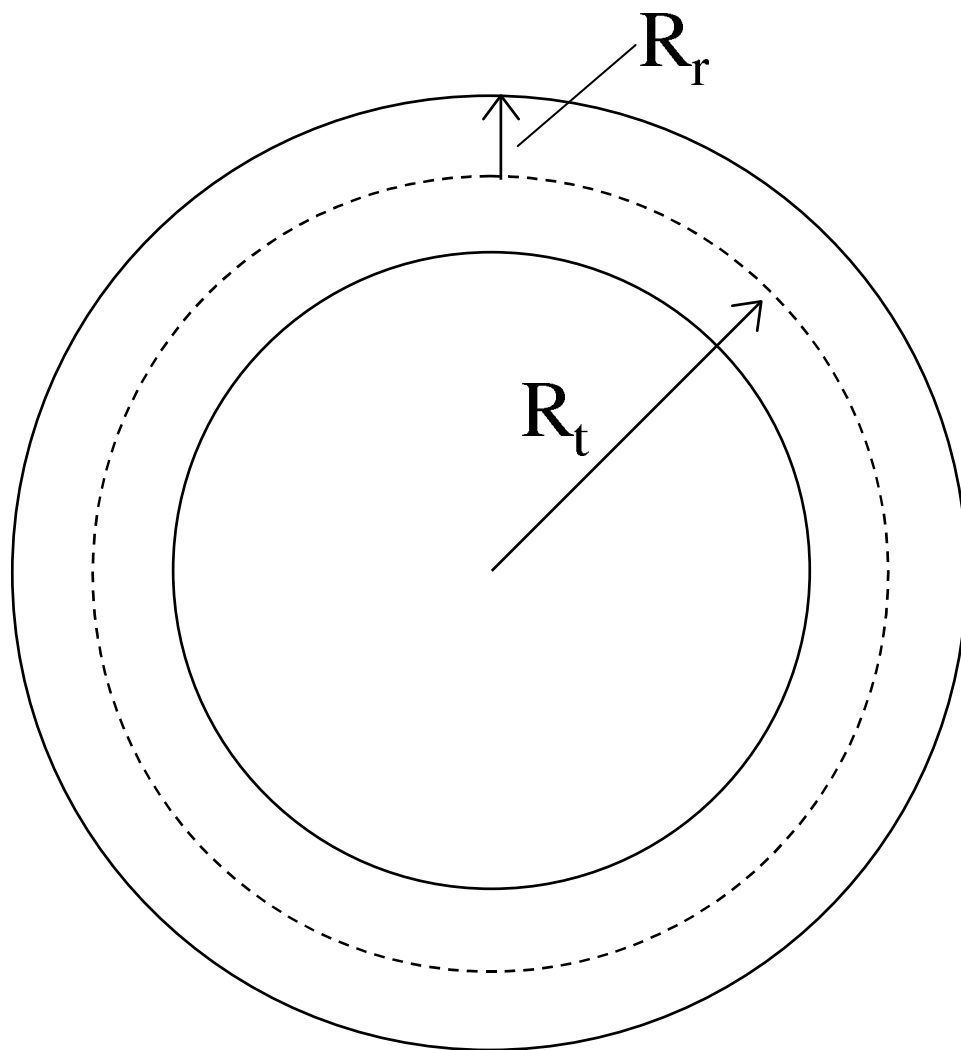


FIG. 4: Cross section of the toroidal DNA globule.

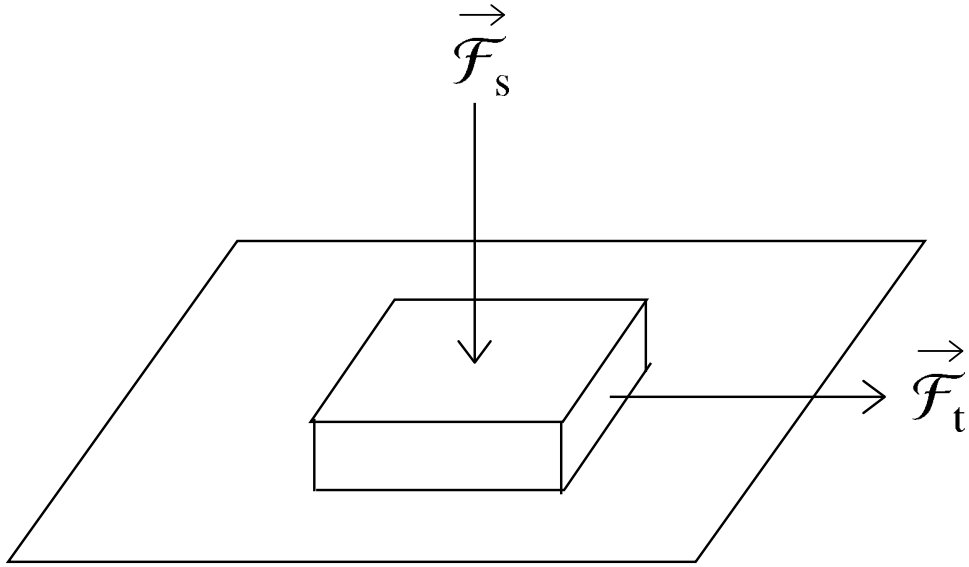


FIG. 5: A standard arrangement to illustrate Coulomb friction.